MOLECULAR AND CELLULAR BIOLOGY, Apr. 2008, p. 2368–2379 Vol. 28, No. 7
0270-7306/08/$08.00+0 doi:10.1128/MCB.01780-07
Copyright © 2008, American Society for Microbiology. All Rights Reserved.

Wnt-3a and Dickkopf-1 Stimulate Neurite Outgrowth in Ewing Tumor Cells via a Frizzled3- and c-Jun N-Terminal Kinase-Dependent Mechanism▽

Yoshimi Endo,[1] Elspeth Beauchamp,[2] David Woods,[1] William G. Taylor,[1] Jeffrey A. Toretsky,[2] Aykut Üren,[2] and Jeffrey S. Rubin[1]*

Laboratory of Cellular and Molecular Biology, National Cancer Institute, National Institutes of Health, Bethesda, Maryland 20892,[1] *and Georgetown University Medical Center, Lombardi Cancer Center, Washington, DC 20057*[2]

Received 27 September 2007/Returned for modification 23 October 2007/Accepted 9 January 2008

Recombinant Wnt-3a stimulated the rapid formation of elongated processes in Ewing sarcoma family tumor (ESFT) cells that were identified as neurites. The processes stained positively for polymerized actin and microtubules as well as synapsin I and growth-associated protein 43. Inhibition of the Wnt receptor, Frizzled3 (Fzd3), with antiserum or by short interfering RNA (siRNA) markedly reduced neurite extension. Knockdown of Dishevelled-2 (Dvl-2) and Dvl-3 also suppressed neurite outgrowth. Surprisingly, disruption of the Wnt/Fzd/lipoprotein receptor-related protein (LRP) complex and the associated β-catenin signaling by treating cells either with the Wnt antagonist Dickkopf-1 (Dkk1) or LRP5/LRP6 siRNA enhanced neuritogenesis. Neurite outgrowth induced by Dkk1 or with LRP5/LRP6 siRNA was inhibited by secreted Fzd-related protein 1, a Wnt antagonist that binds directly to Wnt. Moreover, Dkk1 stimulation of neurite outgrowth was blocked by Fzd3 siRNA. These results suggested that Dkk1 shifted endogenous Wnt activity from the β-catenin pathway to Fzd3-mediated, noncanonical signaling that is responsible for neurite formation. In particular, c-Jun amino-terminal kinase (JNK) was important for neurite outgrowth stimulated by both Wnt-3a and Dkk1. Our data demonstrate that Fzd3, Dvl, and JNK activity mediate Wnt-dependent neurite outgrowth and that ESFT cell lines will be useful experimental models for the study of Wnt-dependent neurite extension.

The Wnts comprise a large family of secreted glycoproteins that have a variety of activities during embryonic development and promote tissue homeostasis in the adult. At the cellular level, Wnts control proliferation, differentiation, survival, motility, and polarity. They also affect the organization of the developing embryo by regulating tissue patterning, organogenesis, and specification of the body plan (43).

Wnts are particularly important in the development of the nervous system, where they are required for several morphogenetic events, including neural tube closure and the formation of specific brain structures as well as induction and migration of neural crest cells (23, 25). Wnt signaling has also been shown to stimulate axonal remodeling, pathfinding, dendritic arborization, and neuronal connectivity in the central nervous system (2, 6, 9, 14, 32, 41, 42). Targeted disruption of the gene encoding the Wnt receptor, Frizzled3 (*Fzd3*), caused severe defects in several major axon tracts of the forebrain, including a complete loss of the thalamocortical, corticothalamic, and nigrostriatal tracts and the anterior commissure as well as variable loss of the corpus callosum (41). Derailed/Ryk, a Wnt-binding atypical receptor tyrosine kinase, regulates axon pathfinding in mammalian systems by eliciting either neurite-repulsive (15, 18, 33) or -attractive (19) responses, depending on the setting. Multiple downstream components of Wnt signaling pathways have been shown to function in neurite outgrowth, although their mechanisms of action have not been fully delineated. The inhibition of glycogen synthase kinase 3β (GSK-3β) by lithium chloride (LiCl) mimics Wnt-7a stimulation of neurite outgrowth, suggesting that Wnt-dependent suppression of GSK-3β activity contributes to neurite extension (14, 20, 21). The activation of Rac1/c-Jun N-terminal kinase (JNK) is associated with Wnt-7b-dependent dendritic arborization in hippocampal neurons (32). Adenomatous polyposis coli (APC) and/or β-catenin has been implicated in neurite outgrowth in rat hippocampal neurons (39, 44) and PC12 cells (39) via a mechanism that differs from the canonical Wnt/β-catenin pathway.

The Ewing sarcoma family of tumors (ESFT) is a group of malignancies characterized by small, round, relatively undifferentiated cells. The ESFT designation includes Ewing sarcoma, primitive peripheral neuroectodermal tumor, neuroepithelioma, atypical Ewing sarcoma, and Askin tumor (8). Although the origin of ESFT cells is uncertain, they exhibit neuronal features (4, 17, 27). Approximately 85% of ESFT tumors result from a specific translocation between chromosomes 11 and 22, t(11, 22), that generates EWS-FLI, a fusion protein containing a member of the Ets family of transcription factors (30). Recent microarray data indicate that ESFT cells have expression patterns that resemble those of neuroectoderm and endothelial cells (36) and that EWS-FLI can induce expression of genes typical of a neural crest phenotype (31). Furthermore, previous studies demonstrated that cyclic AMP, 12-*O*-tetradecanoyl phorbol-13-acetate, and retinoic acid can elicit neuronal characteristics in ESFT cells, including process formation (4, 27). In the present study, we demonstrate that Wnt-3a stimulates neurite outgrowth in multiple ESFT cell lines and identify

* Corresponding author. Mailing address: National Cancer Institute, Bldg. 37, Room 2042, 37 Convent Drive, MSC 4256, Bethesda, MD 20892-4256. Phone: (301) 496-4265. Fax: (301) 496-8479. E-mail: rubinj@mail.nih.gov.

▽ Published ahead of print on 22 January 2008.

mechanisms responsible for this activity. Moreover, we show that the treatment of ESFT cells with Dickkopf-1 (Dkk1), a specific antagonist of the Wnt/β-catenin pathway, also increases neurite outgrowth, apparently by enabling endogenous Wnts to act through similar mechanisms.

MATERIALS AND METHODS

Recombinant proteins. Recombinant Wnt-3a, Wnt-5a, and Dkk1 were purchased from R&D Systems (Minneapolis, MN). Wnt-3a and L conditioned media (CM) were prepared as previously reported (10). Partially purified Wnt-1 was obtained from a Wnt-1 stably transfected Rat-2 fibroblast line kindly provided by Anthony Brown, Cornell Medical Center, New York, NY (13). Rat2/Wnt-1 transfectants were grown in RPMI 1640 culture medium supplemented with 10% fetal bovine serum, 1% streptomycin-penicillin, and 500 μg/ml of G418. Once confluent, the monolayer was maintained in growth medium for 1 week, with fresh medium provided every few days. Then culture fluid was switched to serum-free RPMI 1640 medium, and CM was collected after 72 h. CM was centrifuged (Sorvall RT 7 Plus) at 3,000 rpm for 10 min at 5°C to remove any cell debris. The supernatant was passed through a 0.45-μm nitrocellulose filter and applied to a HiTrap heparin affinity column (1 ml/min; 1-ml bed volume; GE Healthcare, Waukesha, WI), which was equilibrated with 150 mM NaCl/50 mM sodium phosphate buffer, pH 7.4. Bound proteins were eluted by a stepwise increase of NaCl concentration (0.15, 0.3, 0.5, 0.75, and 1 M), 12 ml/step. A small aliquot of each fraction was resolved by sodium dodecyl sulfate-polyacrylamide gel electrophoresis (SDS-PAGE) and analyzed by Western blotting with anti-Wnt-1 antibody. Peak fractions of Wnt-1 were obtained with 0.75 M NaCl. Wnt-1 biological activity was verified by β-catenin stabilization assay using CHO-K1 cells (10).

Recombinant secreted Frizzled-related protein 1 (sFRP-1) was prepared in the lab as described previously (37).

Chemicals. (2′*Z*,3′*E*)-6-Bromoindirubin-3′-oxime (BIO), JNK inhibitor II (SP600125), and JNK inhibitor III (human immunodeficiency virus-$TAT_{47–57}$-gaba-c-Jun$\delta_{33–57}$) were purchased from EMD Chemicals, Inc. (San Diego, CA). LiCl was obtained from Fluka (Buchs, Switzerland).

Antibodies and reagents used for immunostaining. Alexa Fluor 488 phalloidin (catalog no. A12379), Alexa Fluor 568 phalloidin (catalog no. A12389), and mouse anti-α-tubulin antibody (catalog no. A11126) were from Invitrogen (Carlsbad, CA). DAPI (4′,6-diamidino-2-phenylindole) (catalog no. D9542), mouse anti-acetylated tubulin (catalog no. T6793), mouse anti-tyrosinated tubulin (catalog no. T9028), and rabbit anti-Fzd3 antibodies (catalog no. F3179) were purchased from Sigma-Aldrich (St. Louis, MO). Mouse anti-tau antibody (catalog no. 610672) and anti-synapsin I (catalog no. 611392) were from BD Biosciences (San Jose, CA). Rabbit anti-growth associated protein 43 (anti-GAP-43) (catalog no. AB5220) was from Millipore (Billerica, MA).

Antibodies and reagents used for Western blotting. Goat anti-mouse Wnt-1 antiserum (catalog no. AF1620) was from R&D Systems. Mouse anti-Dishevelled-2 (anti-Dvl-2) (catalog no. sc-8026), mouse anti-Dvl-3 (catalog no. sc-8027), and mouse anti-HSP70 (catalog no. sc-7298) antibodies were from Santa Cruz Biotechnology (Santa Cruz, CA). Rabbit anti-JNK/SAPK (catalog no. 9252) and rabbit anti-phospho-JNK/SAPK (Thr183/Tyr185, catalog no. 9251) antibodies were from Cell Signaling Technology, Inc. (Danvers, MA). Rabbit anti-Fzd3 antibody was raised against keyhole limpet hemocyanin-conjugated carboxy-terminal peptide sequence (THGTSMNRVIEEDGTSA) of human Fzd3 and purified with immunoaffinity chromatography, analogous to a previously described protocol (40). Rabbit anti-lipoprotein-receptor-related protein 5 (anti-LRP5) (catalog no. 36-5400) and LRP6 (catalog no. 36-5300) antibodies were from Invitrogen. Mouse anti-JNK-1 (catalog no. 554286) and mouse anti-β-catenin (catalog no. 610154) antibodies were from BD Biosciences.

Antibodies for receptor neutralization experiments. Goat anti-Fzd3 (R&D Systems; catalog no. AF1001), raised against the Fzd3 amino-terminal cysteine-rich domain, and negative control goat immunoglobulin G (IgG) (Santa Cruz Biotechnology, catalog no. sc-2028) were used in blocking experiments. Specificity of the anti-Fzd3 antibody was verified by enzyme-linked immunosorbent assay and Western blotting, as detailed in the product description.

Cell culture. Three ESFT cell lines, TC-32, 5838, and SKES, were maintained in RPMI 1640 medium supplemented with 10% fetal bovine serum, glutamine (2 mM), penicillin (100 U/ml), and streptomycin (100 μg/ml) in a 5% CO_2 humidified 37°C cell culture incubator. ESFT cells were plated on cell culture dishes, cluster plates, or glass coverslips that had been precoated with type I collagen solution (Sigma-Aldrich; catalog no. C8919). Specifically, the surfaces were covered with 0.01% type I collagen (diluted with phosphate-buffered saline [PBS]) and maintained in a cell culture incubator for 1 h. Then the collagen solution was aspirated, surfaces were washed twice with PBS, and cells were plated in RPMI-1640 plus the supplements indicated above (complete RPMI medium).

Immunofluorescent analysis. The ESFT cells were seeded on collagen-coated, 12-mm-diameter glass coverslips (Fisher; catalog no. 12-545-80) in complete RPMI medium. After 24 h, the medium was replaced with Wnt-3a CM or serum-free RPMI 1640 medium containing the indicated recombinant proteins. Cells were incubated for 3 h and then fixed with freshly prepared 3.7% formaldehyde for 15 min at room temperature and permeabilized with 0.1% Triton X-100 in PBS for 5 min. After blocking with 5% bovine serum albumin (BSA) in PBS for 1 h at room temperature, the cells were incubated overnight at 4°C with anti-synapsin I (1:1,000), anti-GAP-43 (1:1,000), anti-Fzd3 (1:2,000), or anti-phospho JNK/SAPK (1:1,000) in 2.5% BSA in PBS, followed by washing three times with PBS and then incubation with 1:1,000-diluted Alexa Fluor 488 goat anti-mouse (catalog no. A11001) or goat anti-rabbit (catalog no. A11008) antibody (Invitrogen) for 30 min at room temperature. Alexa Fluor 568 phalloidin (1:1,000) and DAPI (as indicated) were included during this 30-min period to detect polymerized actin and the nucleus, respectively.

Tubulin staining was performed according to the following procedure. Cells were washed once with PBS and then with PHEM {60 mM Na-PIPES [piperazine-*N*,*N*′-bis(2-ethanesulfonic acid)], 25 mM Na-HEPES, 10 mM Na-EGTA, 2 mM $MgCl_2$, pH 6.9}, followed by treatment with PHEM containing 0.19 M NaCl, 1% saponin, 10 μM Taxol, and 0.1% dimethyl sulfoxide for 5 min at room temperature to extract and stabilize tubulin. Extracted cultures were immersed in methanol at −20°C for 6 min, rehydrated by rinsing in PBS, and treated with blocking solution (5% BSA in PBS) for 10 min at room temperature. Primary antitubulin antibodies (anti-α-tubulin, 1:1,000; anti-acetylated tubulin, 1:4,000; or anti-tyrosinated tubulin, 1:1,600) were added with 2.5% BSA in PBS, and cell samples were incubated for 45 min at 37°C. After washing with blocking solution, cell samples were incubated with the secondary antibody (Alexa Fluor 488 goat anti-mouse IgG, 1:1,000) for 45 min at 37°C.

Cell imaging. Fluorescent images of tubulin and Fzd3 staining were collected with a Zeiss 510 laser scanning confocal microscope by using a 63× objective (Carl Zeiss, Inc., Thornton, NY). Images were captured with an Orca-ERII charge-coupled device camera (Hamamatsu, Bridgewater, NJ). For analysis of other molecules and neurite outgrowth, the images were obtained with an Olympus Vanox epifluorescence microscope by using a 40× objective lens (Olympus, Tokyo, Japan). Images were captured with Photometrics CoolSNAPfx (Roper Scientific, Tucson, AZ). IP Lab software, version 3.6. (BD Biosciences), was used for image processing, and composite figures were prepared with Adobe Photoshop Elements 2.0 (Adobe Systems, Inc., San Jose, CA).

Quantitative analysis of neurite outgrowth. ESFT cells were sparsely seeded on collagen-coated coverslips in a 24-well cell culture plate and maintained in complete RPMI medium. After 24 to 48 h, the medium was replaced with serum-free RPMI 1640 medium containing recombinant proteins or chemicals and cells were incubated for 3 h. After staining with Alexa Fluor phalloidin 488 or 568, cells were visualized under a fluorescence microscope, and 30 to 50 noncontiguous cells corresponding to each treatment group were randomly selected and photographed. The images were processed with Adobe Photoshop Elements 2.0, and the percentage of cells bearing one or more processes that extended at least one cell body length was determined.

RT-PCR. Complementary DNA from ESFT cell lines was synthesized with the SuperScript First-Strand synthesis system for reverse transcriptase PCR (RT-PCR) kit (Invitrogen). Primer sequences for RT-PCR were Fzd3 (forward, 5′-GTGTGTTTTGTCGGCCTCTACG-3′; reverse, 5′-GAATGTGATACTCT CTGCAGCGTTC-3′), Fzd4 (forward, 5′-GCTGGCTTGTACAGCCGCTC-3′; reverse, 5′-TTTGAATAAGGCCACCAAACC-3′), Fzd7 (forward, 5′-GGACC ACGGCTTCTGCCAGC-3′; reverse, 5′-CTGGCCACTGGAAGCCGAAC-3′), Ryk (forward, 5′-AAAGACCTGGCTGCCAGGAAC-3′; reverse, 5′-CCAGGG CTGCATGAAACTCTG-3′), and β-actin (forward, 5′-CCACTGGCATCGTG ATGGAC-3′; reverse, 5′-GCGGATGTCCACGTCACACT-3′). The predicted sizes of PCR products were 313 bp for Fzd3, 624 bp for Fzd4, 299 bp for Fzd7, 434 bp for Ryk, and 428 bp for β-actin. All of the PCR experiments were performed with the following conditions: denaturation at 94°C for 5 min and amplification for 35 cycles, each consisting of incubation at 94°C for 30 s, 58°C for 30 s, and 72°C for 30 or 45 s and extension at 72°C for 8 min. PCR products were verified by DNA sequencing analysis.

siRNA. Double-stranded short interfering RNA (siRNA) reagents directed against Dvl-2, LRP5, LRP6, Fzd3, Fzd4, Fzd7, JNK1, and Ryk were purchased from Dharmacon (Lafayette, CO). Dvl-3 siRNA (target sequence, GCCUAGACGACUUCCACUU) was generated with the Silencer siRNA construction kit from Ambion (Austin, TX). Luc siRNA (target sequence, CGUACGCGGAAUACUUCGA) was synthesized by Dharmacon. All

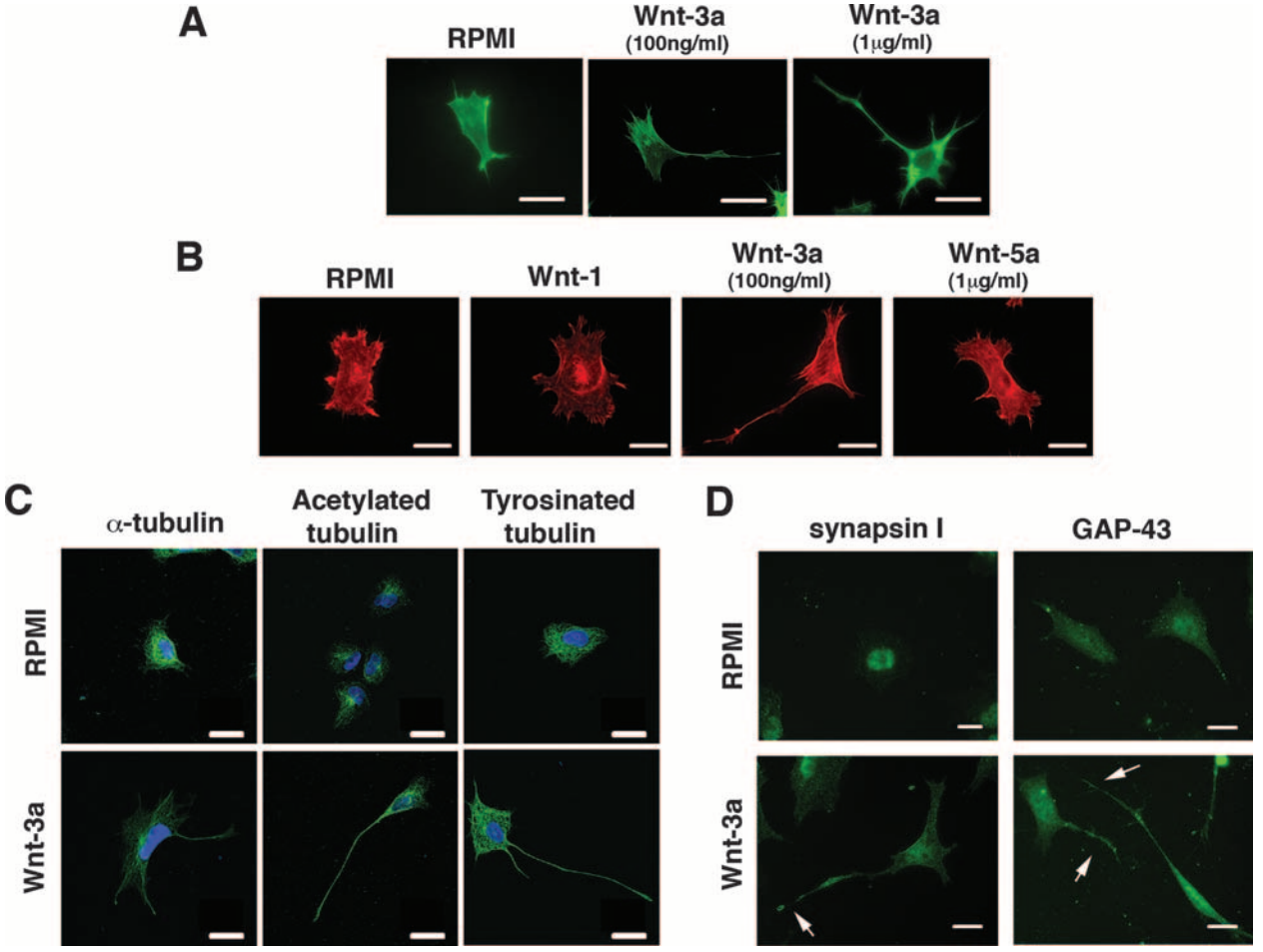

FIG. 1. Wnt-3a stimulated neurite outgrowth in ESFT cell lines. TC-32 cells were seeded on glass coverslips precoated with collagen I and subsequently treated for 3 h with serum-free RPMI medium in the presence or absence of recombinant Wnt-3a. (A) Alexa Fluor 488 phalloidin staining of representative cells from cultures incubated with serum-free RPMI alone (control) or supplemented with Wnt-3a (100 ng/ml or 1 μg/ml). Scale bars, 15 μm. (B) TC-32 cell morphology following treatment with different Wnt ligands. Alexa Fluor 568 phalloidin staining of representative cells from cultures incubated with RPMI (control), partially purified Wnt-1, Wnt-3a (100 ng/ml), or Wnt-5a (1 μg/ml). Scale bars, 20 μm. (C) Staining patterns of anti-α-tubulin, acetylated tubulin, and tyrosinated tubulin in TC-32 cells treated with RPMI control or Wnt-3a (100 ng/ml). Tubulin antibodies stained green; blue (DAPI) stain highlights nuclei. Scale bars, 20 μm. (D) TC-32 cells treated with RPMI medium alone or with Wnt-3a (100 ng/ml) were stained with synapsin I or GAP-43 antibodies. Arrows indicate Wnt-3a-induced neurite outgrowth. Scale bars, 20 μm.

siRNA transfection experiments were performed with the Amaxa system (Amaxa, Cologne, Germany) according to the manufacturer's protocol, using 200 pmol of siRNA/10^6 cells. The effects of siRNA treatment were analyzed 48 h after transfection.

Immunoblotting. To detect β-catenin, Dvl, and JNK, 80 to 90% confluent monolayers of ESFT cells that had been seeded in 6- or 12-well cell culture plates were serum starved overnight. For immunoblot analysis to verify siRNA knockdown of endogenous proteins, ESFT cells transfected with siRNA were seeded in 6- or 12-well cell culture plates and harvested 48 h after transfection. When Dkk1 was used in combination with Wnt, the cells were preincubated with Dkk1 for 30 min at 37°C prior to Wnt treatment. After incubation for the indicated time, cells were rinsed twice with PBS and lysed with buffer containing 50 mM HEPES (pH 7.5), 50 mM NaCl, 1 mM EDTA, 1% Triton X-100, 10 mM sodium pyrophosphate, 50 mM NaF, 1 mM sodium vanadate, 10 μg/ml aprotinin, 10 μg/ml leupeptin, 1 mM phenylmethylsulfonyl fluoride. Cell lysates were clarified by centrifugation at 20,800 × *g* for 10 min at 4°C. The protein concentration was determined with Bio-Rad protein assay reagent (Bio-Rad, Hercules, CA). Samples were diluted in Laemmli buffer, boiled at 95 to 100°C for 10 min, and subjected to SDS-PAGE. To detect Fzd3, samples were incubated at 37°C for 15 min instead of being boiled. For all immunoblotting, 30 μg of protein were loaded per lane in 10% or 4 to 20% polyacrylamide Tris-glycine gels. After SDS-PAGE, the proteins were transferred to Immobilon P membrane (Millipore), which was blocked with 5% milk in T-TBS (20 mM Tris-HCl [pH 8.0], 0.05% Tween 20, 150 mM NaCl), incubated with primary antibody overnight at 4°C, and subsequently incubated with horseradish peroxidase-labeled secondary antibody. The proteins were visualized with SuperSignal Femto chemiluminescent reagents (Pierce, Rockford, IL) by using BioMax films (Eastman Kodak Co., Rochester, NY). For the detection of soluble β-catenin with a glutathione *S*-transferase (GST)-E-cadherin pull-down assay, cell lysates (200 μg) were incubated with GST-E-cadherin fusion protein (5 μg) overnight at 4°C in a rotary shaker, followed by the addition of glutathione agarose beads (catalog no. sc-2009; Santa Cruz Biotechnology) and incubation for 1 or 2 h at 4°C. The beads were spun down and washed three times with cell lysis buffer prior to SDS-PAGE.

To detect phospho-JNK and matching JNK1 protein by immunoblotting, 80 to 90% confluent monolayers of TC-32 cells that had been seeded in collagen-coated 12-well cell culture plates were serum starved overnight. Cells were treated with recombinant Wnt-3a or Dkk1 for indicated times, and washed twice with ice-cold PBS. Then ice-cold cell lysis buffer (20 mM Tris [pH 7.4], 150 mM NaCl, 1 mM EDTA, 1 mM EGTA, 1% Triton X-100, 2.5 mM sodium pyrophosphate, 1 mM β-glycerophosphate, 1 mM sodium vanadate, 10 μg/ml aprotinin, 10 μg/ml leupeptin, 1 mM phenylmethylsulfonyl fluoride, 1× phosSTOP [Roche

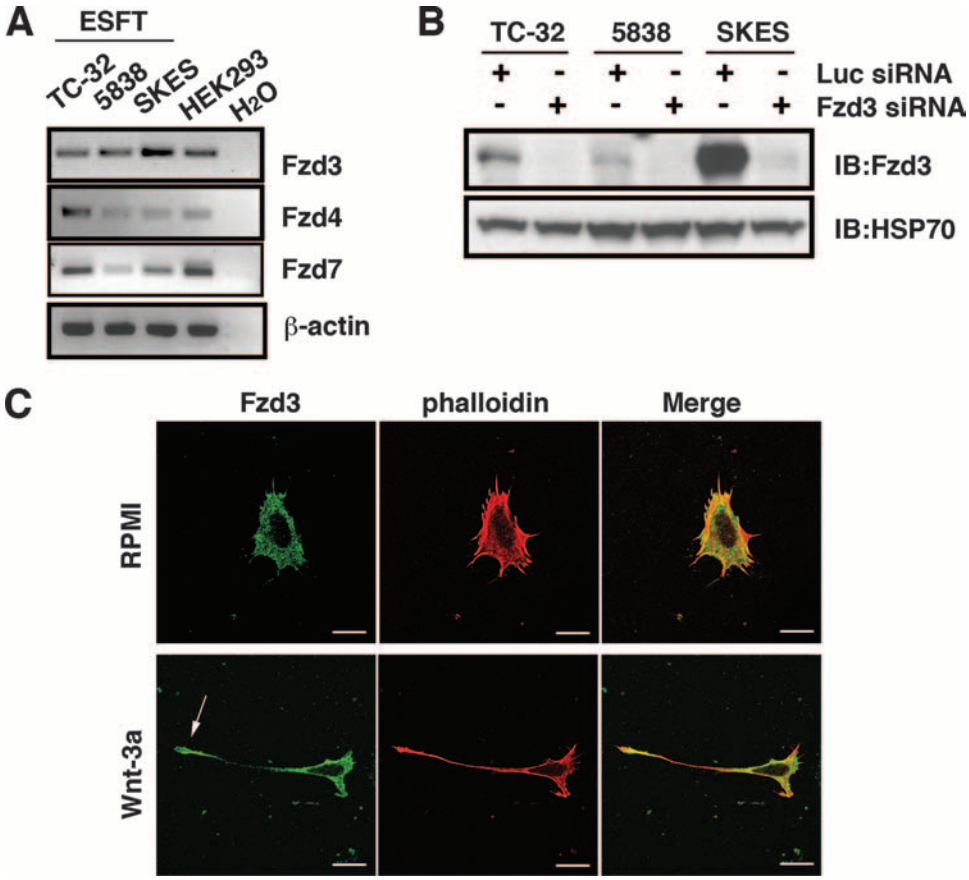

FIG. 2. Fzd3 is expressed in ESFT cell lines. (A) RT-PCR analysis of Fzd expression in three ESFT cell lines. cDNA from HEK293 cells was used as a positive control for Fzd expression. β-Actin RT-PCR was performed as an internal control of RNA analysis. (B) Immunoblot (IB) analysis of Fzd3 protein in three ESFT lines after siRNA treatment. Cells were transfected with either Fzd3 or Luc siRNA, and protein levels were determined 48 h after transfection with Fzd3 antibody raised against a carboxy-terminal peptide of Fzd3. Immunoblotting with anti-HSP70 was performed as a loading control. −, absence of; +, presence of. (C) Immunostaining of Fzd3 in TC-32 cells. TC-32 cells were treated with serum-free RPMI in the presence or absence of Wnt-3a (100 ng/ml) for 3 h and stained with anti-Fzd3 antibody and Alexa Fluor 568 phalloidin. Note prominent Fzd3 staining at the tip of the neurite (arrow). Scale bars, 20 μm.

Applied Science; catalog no. 04 906 837 001]) was added to cells. After incubation on ice for 5 min, cells were harvested and cell lysates were disrupted by passage five times through a 25-gauge needle. Cell lysates were clarified by centrifugation at 14,000 × *g* for 10 min at 4°C. After the protein concentration was determined, 10 μg of protein was loaded per lane in 10% Tris-glycine gels. After SDS-PAGE, protein transfer and immunoblotting were performed as described above.

Neutralization experiments. TC-32 cells that had been plated on collagen-coated glass coverslips were pretreated with either antibody against the amino-terminal extracellular domain of mouse Fzd3 or goat IgG (10 μg/ml) in serum-free RPMI medium for 30 min at 37°C, followed by incubation with or without Wnt-3a (100 ng/ml) for 3 h. Cells were stained with Alexa Fluor 488 phalloidin to evaluate neurite outgrowth.

Statistical analysis. The significance of differences in data obtained from neurite outgrowth assays and densitometry analysis of phospho-JNK was determined with Student's *t* test. The differences were considered to be significant when the *P* value was less than 0.05.

RESULTS

Recombinant Wnt-3a stimulated neurite outgrowth in ESFT cell lines. Earlier we observed that Wnt-3a CM induced the formation of long cytoplasmic extensions in TC-32 cells, an ESFT cell line (38). In the current study, we reproduced these results with purified recombinant Wnt-3a and further characterized the morphological changes. Typically, within 3 h of Wnt treatment, TC-32 cells displayed a single long extension, often bearing one or more small buds, and a few smaller extensions that all contained polymerized actin, as indicated by staining with phalloidin (Fig. 1A). In the absence of Wnt-3a, 10 to 15% of noncontiguous cells exhibited processes greater than one cell diameter in length, whereas exposure to recombinant Wnt-3a (100 ng/ml) increased the percentage of noncontiguous cells with long processes to 50 to 60%. Comparable data were obtained with 1 μg/ml of Wnt-3a (Fig. 1A) and with two other ESFT cell lines, 5838 and SKES (data not shown). In contrast to the case for Wnt-3a, purified recombinant Wnt-5a and partially purified Wnt-1 did not stimulate process formation (Fig. 1B), while they exhibited activity in other assays (data not shown).

To assess the properties of the cellular processes induced by Wnt-3a, we tested the ability of the processes to stain positively for various factors. The TC-32 extensions contained α-tubulin as well as acetylated tubulin and tyrosinated tubulin, the latter two serving as neurite markers (35) (Fig. 1C). The processes also were positive for synapsin I and GAP-43, consistent with a neurite

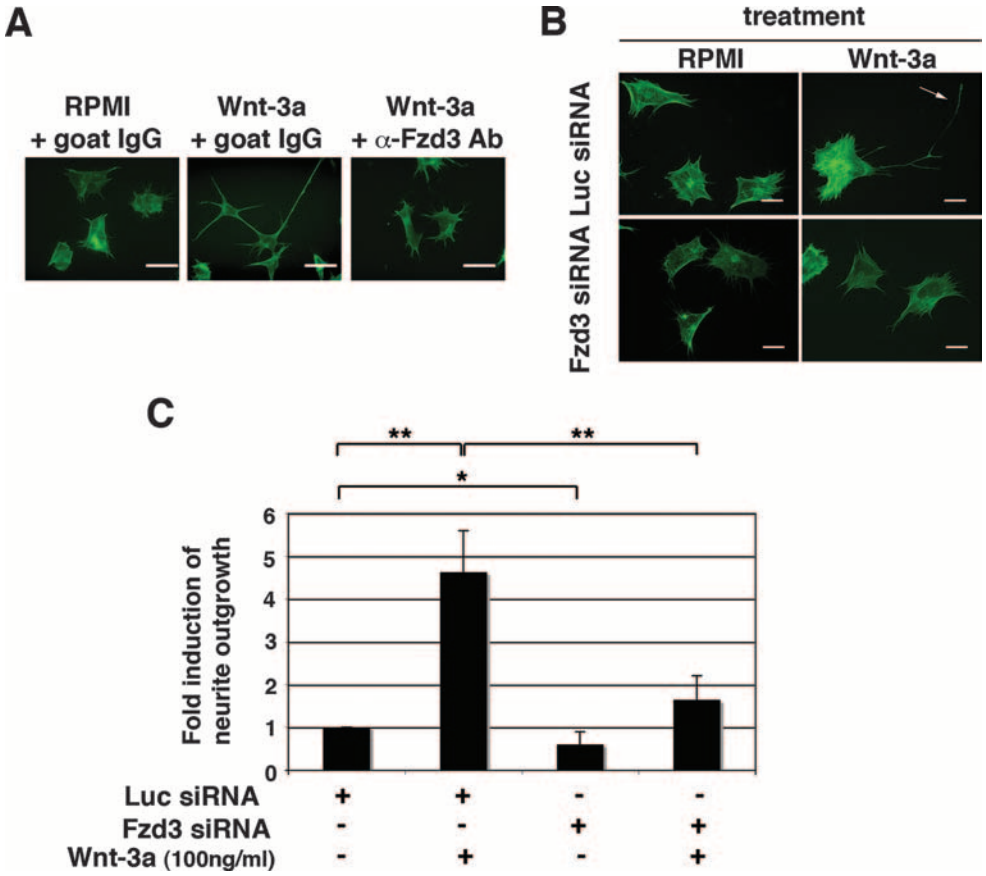

FIG. 3. Fzd3 mediated Wnt-3a-dependent neurite outgrowth. (A) TC-32 cells were pretreated with either antibody against the amino-terminal, extracellular domain of mouse Fzd3 or control goat IgG, followed by incubation with or without Wnt-3a (100 ng/ml) for 3 h. Cell morphology was visualized by Alexa Fluor 488 phalloidin staining. Scale bars, 20 μm. (B) TC-32 cells were transfected with either Fzd3 or Luc siRNA and plated on collagen I-precoated coverslips at sparse density. Approximately 48 h later, cells were treated with serum-free RPMI in the presence or absence of Wnt-3a (100 ng/ml) for 3 h. Cells were then fixed and stained with Alexa Fluor 488 phalloidin. The arrow indicates a branched neurite. Scale bars, 20 μm. (C) Quantitative analysis of the effect of Fzd3 siRNA on neurite outgrowth. The percentage of cells having neurites was determined for each treatment group. The stimulation of neurite outgrowth for each group was defined as the ratio of this percentage to the percentage observed for the Luc siRNA control. The results are means ± standard deviations (error bars) from three independent experiments. −, absence of; +, presence of; *, $P < 0.05$; **, $P < 0.01$.

identity (Fig. 1D). Finally, antibody to tau, a microtubule-associated protein, stained the Wnt-3a-induced extensions in three different ESFT cell lines, whereas it did not stain any cell protrusions in nonneuronal HEK293 cells (data not shown). Taken together, these findings indicated that the Wnt-3a-dependent processes in ESFT cells have the characteristics of neurites.

Fzd3 mediated neurite outgrowth induced by Wnt-3a. As a first step in determining the mechanism of Wnt-3a-induced neurite outgrowth, we analyzed the expression of Wnt receptors in ESFT cells. Using RT-PCR, followed by sequence analysis of PCR products, we established that only Fzd3, Fzd4, and Fzd7 were expressed by all three ESFT lines included in this study (Fig. 2A). (Earlier evidence [38] of Fzd2 expression based on RT-PCR was discounted after sequence analysis.) Because the *Fzd3*-null mouse had major defects in axonal guidance and fiber tracts (41, 42), we initially tested the hypothesis that Fzd3 mediated Wnt-3a-dependent neurite outgrowth in ESFT cells. Fzd3 protein was detected by immunoblotting of ESFT cell lysates (Fig. 2B) and by immunofluorescent analysis, which indicated that Fzd3 was widely distributed in the cell with intense staining at the distal end of the cell extensions (Fig. 2C). When TC-32 cells were treated with antiserum raised against the putative Wnt-binding, amino-terminal, cysteine-rich domain of Fzd3, Wnt-3a-dependent neurite outgrowth was inhibited (Fig. 3A). The result with Fzd3 antibody was reinforced by siRNA knockdown of Fzd3 expression. Compared to the luciferase negative control siRNA, Fzd3 siRNA efficiently blocked the expression of Fzd3 protein (Fig. 2B) and markedly decreased the percentage of cells having long extensions (Fig. 3B and C).

Attempts to analyze the potential contribution of Fzd4 and Fzd7 to neurite outgrowth were hampered by an inability to detect these proteins in ESFT cells with commercially available antisera (data not shown). With the use of siRNA reagents, the expression of *Fzd4* and *Fzd7* transcripts was decreased to an extent similar to that seen with *Fzd3* siRNA (data not shown). Under these conditions, in contrast to the case for Fzd3, there was no significant reduction in the percentage of cells having neurites after treatment with Wnt-3a (data not shown).

Recognizing that Ryk is another Wnt receptor that can me-

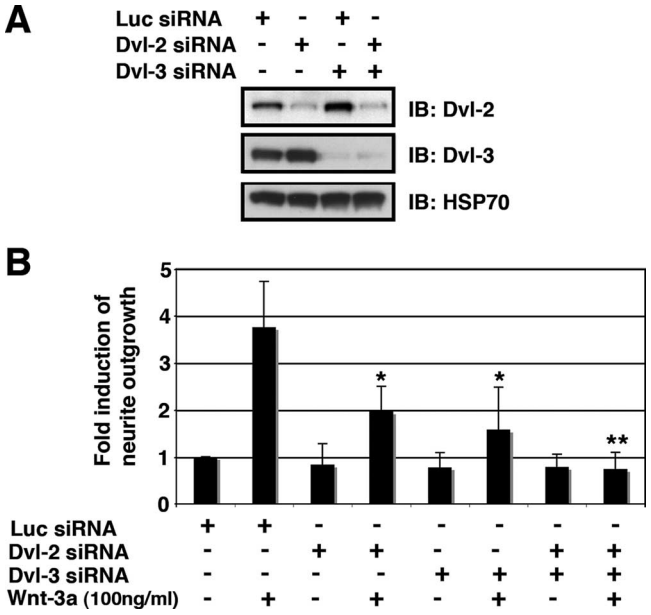

FIG. 4. Dvl-2/Dvl-3 participated in Wnt-3a-induced neurite outgrowth. (A) Single and double knockdown of Dvl-2/Dvl-3 in TC-32 cells. Cells were transfected with Luc, Dvl-2, or Dvl-3 siRNA and incubated for 48 h and the protein levels were analyzed by immunoblotting (IB). (B) Quantitative analysis of the effect of Dvl-2/Dvl-3 siRNA on neurite outgrowth. Approximately 48 h after siRNA transfection, TC-32 cells were treated with serum-free RPMI in the presence or absence of Wnt-3a (100 ng/ml) for 3 h. The percentage of cells having neurites was determined for each treatment group. The stimulation of neurite outgrowth for each group was defined as the ratio of this percentage to the percentage observed for the Luc siRNA control. The results are means ± standard deviations (error bars) from three independent experiments. Asterisks indicate statistical significance in comparison with the Luc siRNA-transfected, Wnt-3a-treated group. −, absence of; +, presence of; *, $P < 0.05$; **, $P < 0.01$.

diate Wnt-3a-dependent neurite outgrowth (19), we examined its potential role in ESFT process formation. Ryk transcript was detected in all three ESFT lines, although the protein was not visualized by immunoblotting with commercial antiserum (data not shown). Neither antiserum raised against its extracellular domain nor Ryk siRNA blocked Wnt-3a-induced neurite outgrowth (data not shown). Thus, we concluded that Fzd3 was the primary receptor transducing the Wnt signal responsible for neurite extension in ESFT cells.

Dvl-2/Dvl-3 participated in Wnt-3a-dependent neurite outgrowth. Dvl proteins are critical effector molecules in multiple Wnt signaling pathways (24) and have been implicated in Wnt-dependent dendritic arborization (32). In ESFT cells, Dvl-2 and Dvl-3 were detected by immunoblotting, but Dvl-1 was not observed (Fig. 4A and data not shown). To test whether Dvl-2 and/or Dvl-3 were required for Wnt-3a-dependent neurite outgrowth, we used siRNA to knock down the expression of Dvl isoforms individually or in combination. Specific knockdown of either Dvl-2 or Dvl-3 alone partially inhibited neurite outgrowth, while double knockdown of Dvl-2/Dvl-3 almost completely blocked the formation of long neurites (Fig. 4A and B). These results indicated that each of the Dvl proteins contributed to Wnt-dependent extension of processes and that together they were essential for neuritogenesis.

Dkk1 treatment and LRP5/LRP6 siRNA stimulated neurite outgrowth. To investigate the signaling mechanisms responsible for Wnt-3a-dependent neurite outgrowth, we next examined the effect of Wnts on the β-catenin pathway. Normally in the absence of Wnt stimulation, a cytoplasmic multiprotein assembly that includes Axin, APC, casein kinase I α (CKIα), and GSK-3 facilitates the phosphorylation of β-catenin by CKIα and GSK-3, targeting it for rapid proteasomal degradation. Signaling through the β-catenin pathway requires Wnt association with both a Fzd and a member of the LRP family, either LRP5 or LRP6. Wnt/Fzd/LRP binding disrupts the Axin-based, β-catenin destruction complex, interfering with phosphorylation by CKIα and GSK-3. Consequently, β-catenin accumulates in the cytosol and ultimately the nucleus, where it promotes the expression of Wnt target genes (7).

Wnt-3a and Wnt-1 both increased the amount of soluble β-catenin in TC-32 cells (Fig. 5A). However, Wnt-1 did not enhance neurite formation (Fig. 1B). Thus, the activation of the β-catenin pathway was not sufficient for neuritogenesis, but it still might be required for neurite outgrowth. To address this possibility, we treated TC-32 cells with Dkk1, a specific antagonist of Wnt/β-catenin signaling that binds directly to LRP5/LRP6 and prevents formation of the Wnt/Fzd/LRP complex (26). As shown in Fig. 5B, preincubation of cells for 30 min with Dkk1 (1 μg/ml) dramatically reduced the accumulation of free β-catenin, confirming that Dkk1 inhibited the β-catenin pathway in our model system. However, we observed that Dkk1 failed to block Wnt-3a-dependent neurite outgrowth, demonstrating that disruption of the Axin/APC/GSK-3/β-catenin destruction complex was not required for neurite extension (Fig. 5C and D). Surprisingly, Dkk1 treatment alone increased the proportion of cells with neurites from 10 to 15% to 30 to 35% in the absence of exogenous Wnt-3a (Fig. 5C and D). While the percentage of cells with long neurites in response to Dkk1 tended to be somewhat lower than that seen with an optimal concentration of Wnt-3a, qualitatively, the effects were comparable.

The unexpected stimulation of neurite outgrowth by Dkk1 raised questions about its mechanism of action. As noted above, Dkk1 is both a ligand for LRP5/LRP6 and a specific antagonist of the Wnt/β-catenin pathway. Although it has not been reported to signal through either LRP5 or LRP6, Dkk2 has been shown to have a stimulatory effect on the Wnt/β-catenin pathway (26). To rule out the possibility that the increase in neurite outgrowth elicited by Dkk1 was mediated by LRP5/LRP6, we repeated the experiment after knocking down expression of the receptors with siRNA reagents. While protein levels of LRP5/LRP6 were reduced by siRNA (Fig. 5E), this reduction did not impair the neurite-promoting effects of Dkk1 (Fig. 5F). Rather, LRP5/LRP6 siRNA treatment also stimulated neurite outgrowth to a degree equivalent to that observed in response to Dkk1 (Fig. 5F). These results established that the Wnt coreceptors and Dkk1 binding partners, LRP5/LRP6, were not required for Dkk1-induced neurite outgrowth. Moreover, the inhibition of LRP5 and LRP6 signaling, either by the addition of Dkk1 or by siRNA suppression of their expression, promoted neurite extension.

Dkk1- and LRP5/LRP6 siRNA-induced neurite outgrowth were blocked by sFRP-1. Because the addition of Dkk1 and knockdown of LRP5/LRP6 both mimicked Wnt-3a stimulation

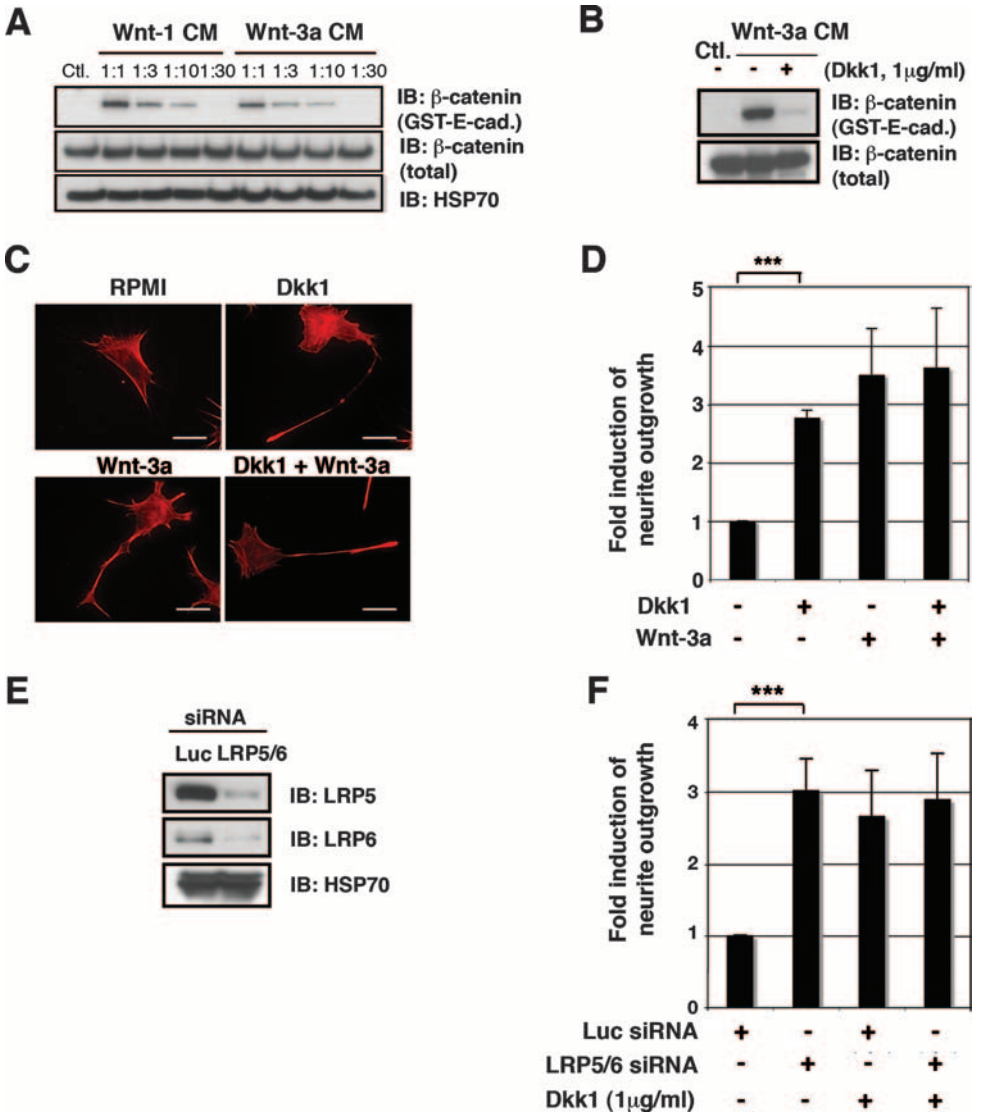

FIG. 5. Dkk1 treatment and LRP5/LRP6 siRNA stimulated neurite outgrowth. (A) Wnt-1 and Wnt-3a CM promoted β-catenin stabilization in TC-32 cells. Stabilization of free β-catenin was analyzed by GST-E-cadherin pull-down assay. Immunoblot (IB) analyses of β-catenin pelleted with GST-E-cadherin and of β-catenin and HSP70 in whole-cell lysates are indicated. −, absence of; +, presence of. (B) Dkk1 blocked Wnt-3a-induced β-catenin stabilization in TC-32 cells. Cells were serum starved overnight and pretreated with Dkk1 for 30 min at 37°C in a CO_2 incubator. Wnt-3a CM or control L (Ctl.) CM were then added, and cells were further incubated for 3 h, followed by GST-E-cadherin pull-down assay. (C) Dkk1 induced neurite outgrowth. TC-32 cells plated on coverslips were pretreated with Dkk1 as indicated and subsequently incubated with Wnt-3a or control medium for 3 h. Then cells were fixed and stained with Alexa Fluor 568 phalloidin. Scale bars, 20 μm. (D) Quantitative analysis of the effect of Dkk1, Wnt-3a, and cotreatment with Dkk1 and Wnt-3a on neurite outgrowth. The percentage of cells having neurites was determined for each treatment group. The stimulation of neurite outgrowth for each group was defined as the ratio of this percentage to the percentage observed for the negative control. The results are means ± standard deviations (error bars) from three independent experiments. ***, $P < 0.001$. (E) Knockdown of LRP5 and LRP6 in TC-32 cells. Cells were transfected with either Luc siRNA or LRP5 and LRP6 siRNA. Cells were harvested 48 h later, and LRP5/LRP6 immunoblotting was performed, along with HSP70 analysis. (F) Quantitative analysis of the effect of LRP5/LRP6 knockdown on neurite outgrowth. Approximately 48 h after the transfection of siRNA, TC-32 cells were treated with serum-free RPMI in the presence or absence of Dkk1 for 3 h. The percentage of cells having neurites was determined for each treatment group. The stimulation of neurite outgrowth for each group was defined as the ratio of this percentage to the percentage observed for the Luc siRNA control. The results are means ± standard deviations (error bars) from three independent experiments. Note that Dkk1 did not further induce neurite outgrowth when LRP5/LRP6 was knocked down. −, absence of; +, presence of; ***, $P < 0.001$.

of neurite outgrowth, we reasoned that endogenous Wnts might account for their activity. The multiplicity of Wnts expressed by TC-32 cells (38) as well as the limited availability and sensitivity of antisera to these Wnts hampered our analysis. Therefore, we tested the hypothesis by assessing the ability of the Wnt-binding antagonist, sFRP-1, to block neurite extension induced by Dkk1 or LRP5/LRP6 siRNA. Recombinant sFRP-1 markedly reduced neurite outgrowth observed in response to both Dkk1 and knockdown of LRP5/LRP6 (Fig. 6A and B). As a control for sFRP-1 activity, we made use of the

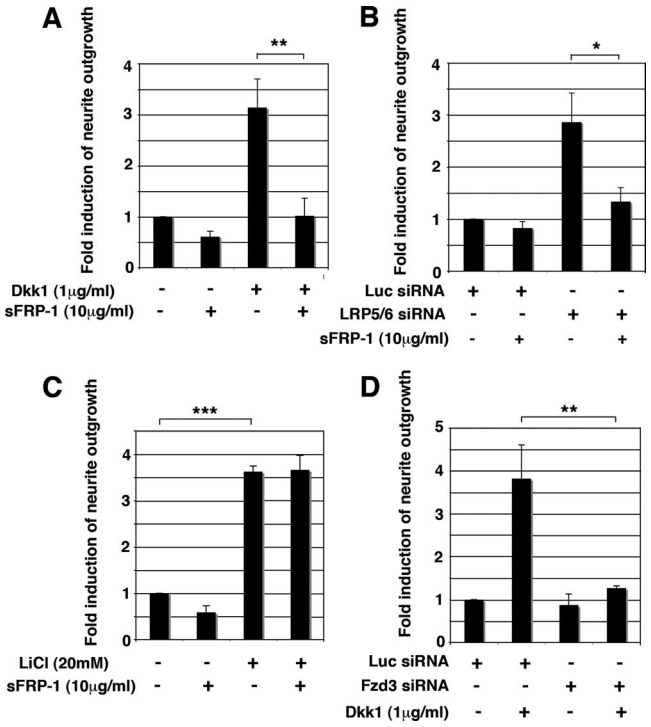

FIG. 6. Dkk1-induced neurite outgrowth and LRP5/LRP6 siRNA-induced neurite outgrowth were blocked by sFRP-1. (A) sFRP-1 blocked Dkk1-induced neurite outgrowth. TC-32 cells plated on coverslips were pretreated with sFRP-1 (10 μg/ml) for 30 min at 37°C in a CO_2 incubator and subsequently incubated in the presence or absence of Dkk1 (1 μg/ml) for 3 h. Quantitative analysis of neurite outgrowth was performed as described for Fig. 5C. The results are means ± standard deviations (error bars) from three independent experiments. **, $P < 0.01$. (B) sFRP-1 blocked LRP5/LRP6 siRNA-induced neurite outgrowth. TC-32 cells were transfected with LRP5/LRP6 or Luc control siRNA and were plated on coverslips. Approximately 48 h after transfection, medium was replaced with serum-free RPMI with or without sFRP-1 (10 μg/ml), and cells were then incubated for 6 h at 37°C in a CO_2 incubator. Quantitative analysis of neurite outgrowth was performed as described for Fig. 5F. The results are means ± standard deviations (error bars) from three independent experiments. *, $P < 0.05$. (C) The effect of sFRP-1 on LiCl-stimulated neurite outgrowth. TC-32 cells plated on coverslips were pretreated with sFRP-1 (10 μg/ml) for 30 min at 37°C in a CO_2 incubator and further incubated with LiCl (20 mM) or negative control NaCl (20 mM) in serum-free RPMI for 3 h. The percentage of cells having neurites was determined for each treatment group. The stimulation of neurite outgrowth for each group was defined as the ratio of this percentage to the percentage observed for the NaCl control. The results are means ± standard deviations (error bars) from three independent experiments. ***, $P < 0.001$. (D) Fzd3 siRNA blocked Dkk1-dependent neurite extension. TC-32 cells were transfected with Fzd3 siRNA and plated on coverslips. Approximately 48 h after transfection, medium was replaced with serum-free RPMI with or without Dkk1 (1 μg/ml) and cells were incubated for an additional 3 h. The results are means ± standard deviations (error bars) from three independent experiments. −, absence of; +, presence of; **, $P < 0.01$.

observation that GSK-3 inhibitors, such as LiCl and BIO, induced neurite outgrowth in TC-32 cells (Fig. 6C and data not shown), as documented for many neuronal models (14, 20, 21, 46). In contrast to the neurite-promoting effects of Dkk1 and LRP5/LRP6 siRNA, sFRP-1 did not block neurite extension triggered by LiCl (Fig. 6C). This result indicated that the inhibitory effect of sFRP-1 was restricted to specific stimuli and was consistent with the supposition that it was attributable to the antagonism of endogenous Wnt/Fzd signaling. Further support for this idea came from experiments demonstrating that neurite outgrowth induced by Dkk1 was almost completely eliminated by knockdown of Fzd3 (Fig. 6D). Taken together, these findings strongly suggested that Dkk1 stimulated neurite outgrowth through a Wnt/Fzd-dependent mechanism.

JNK mediated Wnt-3a-dependent and Dkk1-dependent neurite outgrowth in ESFT cells. JNK is a well-established downstream effector of Wnt/noncanonical signaling in the convergent extension/planar cell polarity pathway (34). It also has been identified as a key mediator of neurite outgrowth (11, 28), specifically functioning in Wnt-7b-dependent, Dvl/Rac-mediated dendritic arborization (32). To examine the potential role of JNK in Wnt-dependent neurite outgrowth, we first sought evidence of the activation of JNK following the exposure of TC-32 cells to Wnt-3a. We observed a small but statistically significant increase in phosphorylated JNK, indicative of activation (Fig. 7A and B). Moreover, Dkk1 treatment also was associated with a transient elevation in phospho-JNK signal by immunoblotting (Fig. 7A and B). Of note, the magnitude of the activation of JNK following exposure to either Wnt-3a or Dkk1 was reduced if Fzd3 expression was concomitantly diminished by siRNA (data not shown). We also examined the intracellular distribution of phosphorylated JNK in TC-32 cells following the addition of Wnt-3a or Dkk1. After 1 h of treatment with either recombinant Wnt-3a or Dkk1, phospho-JNK staining was observed primarily in the nuclear/perinuclear region but was also detected at the tip of the neurites (Fig. 7C). These data provided evidence that Wnt-3a and Dkk1 activated JNK in TC-32 cells and that this signaling might contribute to neurite outgrowth.

To investigate the relevance of JNK activity, we tested the ability of JNK inhibitors to block neurite outgrowth induced by Wnt-3a or Dkk1. Using two structurally unrelated antagonists that act through different mechanisms, JNK inhibitor II (SP600125) and JNK inhibitor III (human immunodeficiency virus-$TAT_{47–57}$-gaba-c-Jun$\delta_{33–57}$), we observed that each antagonist decreased the percentage of cells with long neurites following treatment with either Wnt-3a or Dkk1 (Fig. 8A and B). To reinforce the credibility of these findings, we inhibited JNK expression with siRNA. In particular, we chose to target the expression of the JNK1 isoform because the phosphorylated JNK band we detected by immunoblotting corresponded in size to JNK1. After verifying that siRNA reagents markedly suppressed JNK1 protein expression (Fig. 8C), we determined that both Wnt-3a-dependent and Dkk1-dependent neurite outgrowth were significantly reduced by knockdown of JNK1 (Fig. 8D). Taken together, our results strongly suggest that Wnt-3a and Dkk1 stimulate neurite extension in ESFT cells by one or more mechanisms that involve Fzd3 and JNK1.

DISCUSSION

In this report, we identified ESFT cells as a new model system for the study of Wnt-dependent neurite outgrowth. Several articles have established that Wnt signaling stimulates axonal guidance and dendritic arborization in vivo, in organ

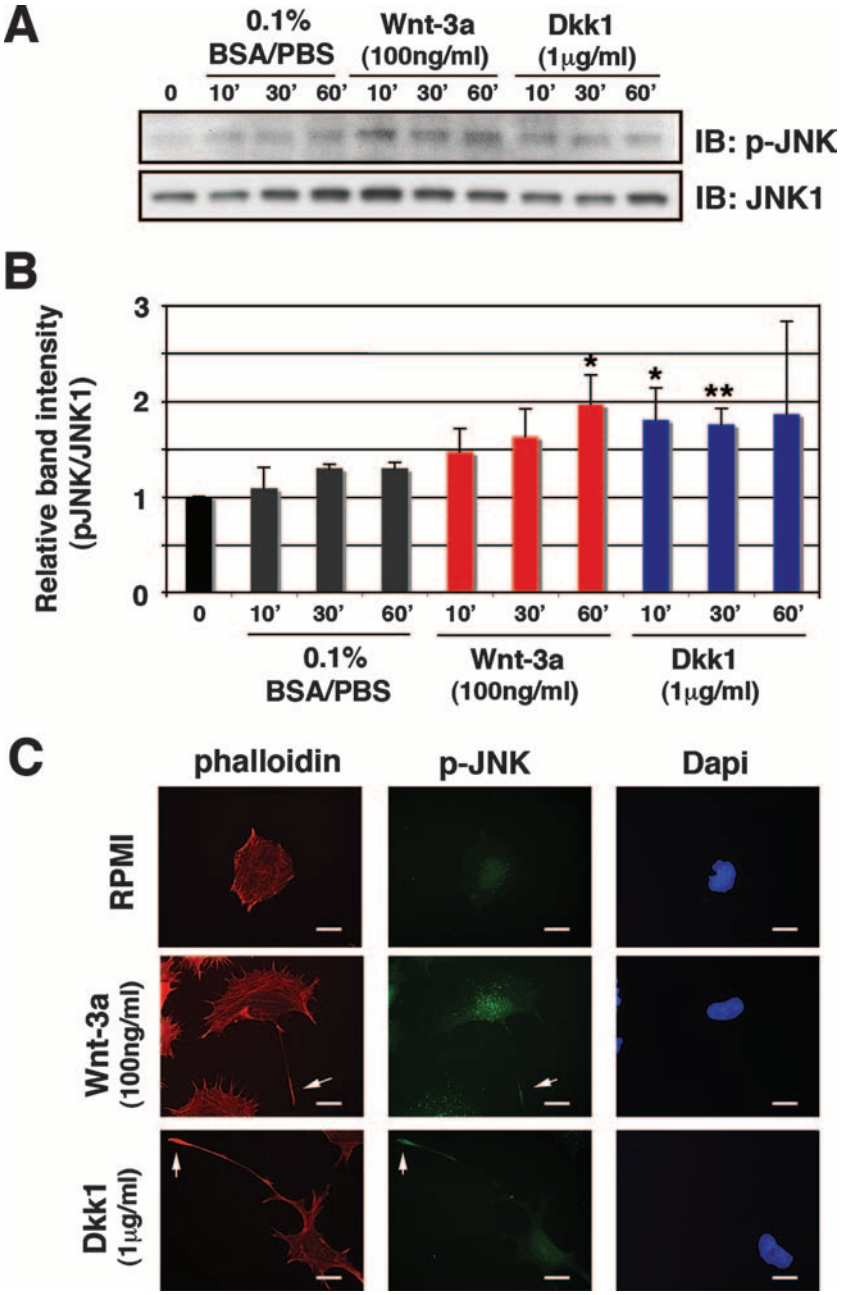

FIG. 7. Wnt-3a and Dkk1 stimulated JNK phosphorylation. (A) Wnt-3a and Dkk1 induced JNK phosphorylation. TC-32 cells were serum starved overnight and treated with Wnt-3a (100 ng/ml), Dkk1 (1 μg/ml), or vehicle control (0.1% BSA-PBS) for 10, 30, or 60 min. Phosphorylated JNK and total JNK1 were analyzed by immunoblotting. The panels show representative data from one of three independent experiments. (B) Quantitative analysis of the effect of Wnt-3a and Dkk1 on JNK phosphorylation. The band intensity of p-JNK was normalized to each corresponding band of the JNK1 blot, and relative band intensity was defined as the ratio of this normalized value to the normalized value of the time zero control. The results are means ± standard deviations (error bars) from three independent experiments. Asterisks indicate statistical significance in a comparison of each time point with the corresponding 0.1% BSA-PBS control. *, $P < 0.05$; **, $P < 0.01$. (C) Immunostaining of p-JNK in TC-32 cells. Cells sparsely plated on precoated coverslips were treated with Wnt-3a (100 ng/ml) or Dkk1 (1 μg/ml) for 1 h, fixed, and stained with anti-p-JNK antibody, Alexa Fluor 568 phalloidin and DAPI. Note prominent p-JNK staining at the tip of the neurites (arrows). Scale bars, 20 μm.

culture and in primary neuronal cell culture (2, 6, 14, 15, 18–21, 32, 33, 41, 42). However, in cell lines that have been used to investigate neurite outgrowth, such as the PC12 rat pheochromocytoma line or the Neuro2A neuroblastoma line, Wnt treatment either induced neurite retraction (PC12) (16) or had no effect (Neuro2) (29). In contrast, ESFT cells responded promptly to Wnt-3a, extending multiple processes, often with a predominant one greater than a cell diameter in length, within 3 h. The ease of handling these cell lines, combined with the efficacy of manipulation with siRNA reagents, indicates that

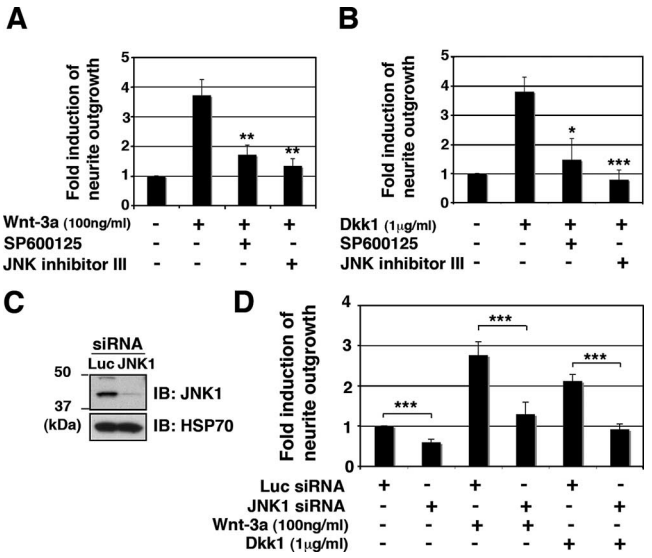

FIG. 8. JNK inhibition blocked neurite outgrowth induced by Wnt-3a or Dkk1. TC-32 cells sparsely plated on precoated coverslips were pretreated with JNK inhibitor II (SP600125) (10 μM) or JNK inhibitor III (100 μM) for 30 min in serum-free RPMI, and subsequently incubated for 3 h in the presence or absence of Wnt-3a (A) or Dkk1 (B). Cells were then fixed and stained with Alexa Fluor 488 phalloidin. The percentage of cells having neurites was determined for each treatment group. The stimulation of neurite outgrowth for each group was defined as the ratio of this percentage to the percentage observed for the negative control. The results are means ± standard deviations (error bars) from three independent experiments. *, $P < 0.05$; **, $P < 0.01$; ***, $P < 0.001$. (C) siRNA knockdown of JNK1 in TC-32 cells. Cells were transfected with Luc or JNK1 siRNA, and knockdown of protein levels was analyzed 48 h later by immunoblotting (IB), including HSP70. (D) TC-32 cells transfected with Luc or JNK1 siRNA were plated on coverslips. Approximately 48 h later, cells were treated with serum-free RPMI in the presence or absence of Wnt-3a or Dkk1 for 3 h. The stimulation of neurite outgrowth for each group was defined as the ratio of this percentage to the percentage observed for the negative control. The results are means ± standard deviations (error bars) from three independent experiments. −, absence of; +, presence of; ***, $P < 0.001$.

ESFT cells will be particularly useful in defining the mechanisms of neurite outgrowth elicited by Wnts.

Fzd3 was a primary mediator of Wnt-dependent neurite formation in the TC-32 cell line. While Fzd3 protein was broadly distributed in cells, intense immunostaining was seen at the distal ends of long neurites and inhibition of its function either with Fzd3 antiserum or siRNA knockdown blocked the growth of these processes. The magnitude of inhibition observed with these reagents demonstrated that Fzd3 has a predominant role in Wnt-induced neurite extension in these cells. Negative data with Fzd4, Fzd7, and Ryk siRNA reagents and Ryk antiserum suggested that they had little or no effect on process formation. Our findings provided direct evidence in support of observations made with *Fzd3*-null mice that Fzd3 is critical for axonal growth and guidance (41, 42). A gradient distribution of endogenous or ectopically expressed Wnt-4 was implicated in the Fzd3-dependent anterior movement of commissural axons after they cross the midline (22). Here we used a purified, recombinant reagent to demonstrate that Wnt-3a also signals through Fzd3 to promote neurite outgrowth. Sequence analysis revealed that Wnt-3a and Wnt-4 are closely related to each other (24), so it is not surprising that they trigger similar biological responses through the same Fzd receptor.

Dvl proteins are key effectors of multiple Wnt signaling pathways (24) and have been implicated in axonal specification and neurite outgrowth (12, 45). Thus, our finding that Dvl knockdown blocked Wnt-3a-dependent neurite outgrowth in TC-32 cells was complementary to earlier work. It was noteworthy that partial inhibition of neurite extension was achieved by reducing the expression of either Dvl-2 or Dvl-3 and that complete inhibition required the simultaneous suppression of both isoforms. This result demonstrated that both Dvl-2 and Dvl-3 participated in the signaling mechanisms responsible for neurite extension and that the magnitude of the response to Wnt-3a was dependent on their combined presence. It is possible that Dvl-2 and Dvl-3 have nonredundant roles, or they may function interchangeably and their combined concentration determines the extent of neurite outgrowth. In comparison, Dvl-1 is the only isoform expressed in rat hippocampal neurons, where it promotes axonal specification (45). These findings imply that all three Dvl isoforms contribute to axonal specification and/or extension, although their particular functions depend on their individual expression patterns and perhaps specific mechanistic differences yet to be elucidated.

The ability of Dkk1 to promote neurite formation was unexpected and warranted further investigation. Dkk1 has been viewed primarily as a specific inhibitor of the canonical Wnt/β-catenin pathway (26); how it mimicked Wnt activity on neurite outgrowth was the question. We excluded the possibility that it signaled through its binding partners, the Wnt coreceptors LRP5/LRP6, by knocking down their expression with siRNA reagents. This manipulation did not prevent neurite outgrowth in response to recombinant Dkk1. Rather, LRP5/LRP6 knockdown had an effect similar to that of Dkk1: a moderate stimulation of neurite extension. To explain these observations, we propose that both Dkk1 treatment and LRP5/LRP6 silencing promote neuritogenesis by shifting endogenous Wnts from Wnt/Fzd/LRP complexes to Wnt/Fzd interactions that transduce the noncanonical signaling responsible for neurite formation. In support of this notion, sFRP-1 inhibited neurite formation stimulated by Dkk1 or LRP5/LRP6 siRNA and Fzd3 siRNA also blocked Dkk1-induced neuritogenesis. Our previous work indicated that ESFT cells contain various Wnt transcripts, with Wnt-10b being the one most commonly expressed (38). Subsequent experiments have shown that CM from a cell line expressing recombinant Wnt-10b has potent activity in the neurite outgrowth assay (unpublished observations). Thus, we hypothesize that Dkk1 enhances the activity of endogenous Wnts, such as Wnt-10b, to increase the percentage of cells with long neurites. While the present study has not provided a complete account of the mechanisms that mediate neurite formation, the activation of JNK appears to have a significant role in the responses to both exogenous Wnt-3a and Dkk1. Of note, Dkk1 was reported to stimulate JNK activity in other contexts, either independent of, or while suppressing, canonical Wnt signaling (3, 26). Moreover, Dkk1 increased the motility of CHO-K1 cells in the absence of exogenous Wnt, presumably via noncanonical signaling (10). In summary, we surmise that Dkk1 functions not only as an antagonist of the

Wnt/β-catenin pathway but also as an agent that can upregulate other Wnt signaling pathways if the requisite Wnt/receptor combinations are available.

Several lines of evidence indicate that JNK signaling is important for Wnt-dependent neurite outgrowth in ESFT cells. Both Wnt-3a and Dkk1 stimulated an increase in phospho-JNK, indicative of activation. While the magnitude of this effect was not large, it was comparable to the level of JNK stimulation previously seen in the context of Wnt-dependent neurite extension (32). Although immunostaining revealed that the vast majority of phospho-JNK was located in the nucleus or perinuclear region, signal also was detected at the tips of neurites following Wnt-3a or Dkk1 treatment. At this location, activated JNK could have a direct effect on neurite outgrowth by phosphorylating substrates involved in regulating cytoskeletal extension, such as MAP-1B, MAP-2, and tau (1, 5). Two structurally unrelated JNK antagonists, a competitive inhibitor targeting the ATP binding site and a peptide that disrupts JNK/substrate interaction, each abrogated neurite formation induced by Wnt-3a or Dkk1. These results were reinforced when similar data were obtained following siRNA knockdown of JNK1. Others have shown that the activation of JNK is required for neurite outgrowth in dopaminergic (11) and hippocampal (28, 32) neurons. *Jnk1*$^{-/-}$ mice had severe defects in the anterior commissure tract and a progressive loss of microtubules within axons and dendrites (5), demonstrating that JNK1 is required for the maintenance of neuronal microtubules. Furthermore, *Fzd3*$^{-/-}$ mice also were characterized by a complete loss of the anterior commissure, suggesting a functional connection between Fzd3 and JNK1. Similarly, our observations that Fzd3 RNA interference appeared to decrease the activation of JNK1 by Wnt-3a and Dkk1 gave additional support for the idea that JNK is downstream of Fzd3.

In conclusion, we have shown that recombinant Wnt-3a stimulates neurite outgrowth in ESFT cell lines. Fzd3 is the primary receptor that mediates this activity, and both Dvl-2 and Dvl-3 serve as downstream effectors. Dkk1 promotes neurite outgrowth in ESFT cells, apparently by shifting endogenous Wnts from stimulation of the β-catenin pathway to noncanonical signaling. The activation of JNK appears to be an important component of both Wnt-3a and Dkk1 activity. GSK-3 inhibition also stimulates neurite outgrowth in ESFT cells, although its potential role and mechanism in Wnt-dependent neurite outgrowth have not been established. The ESFT cell lines should prove useful in the further elucidation of mechanisms that play a role in Wnt-dependent neurite outgrowth.

ACKNOWLEDGMENTS

We thank Anthony Brown for the Rat2 fibroblast/Wnt-1 transfectant line, members of the Rubin laboratory for helpful discussions, and Matthew W. Kelley and Alain Dabdoub for comments about the manuscript.

This research was supported by the Intramural Research Program of the National Institutes of Health, National Cancer Institute.

REFERENCES

1. **Bogoyevitch, M. A., and B. Kobe.** 2006. Uses for JNK: the many and varied substrates of the c-Jun N-terminal kinases. Microbiol. Mol. Biol. Rev. **70:** 1061–1095.
2. **Bovolenta, P., J. Rodriguez, and P. Esteve.** 2006. Frizzled/RYK mediated signalling in axon guidance. Development **133:**4399–4408.
3. **Caneparo, L., Y. L. Huang, N. Staudt, M. Tada, R. Ahrendt, O. Kazanskaya, C. Niehrs, and C. Houart.** 2007. Dickkopf-1 regulates gastrulation movements by coordinated modulation of Wnt/beta catenin and Wnt/PCP activities, through interaction with the Dally-like homolog Knypek. Genes Dev. **21:**465–480.
4. **Cavazzana, A. O., J. S. Miser, J. Jefferson, and T. J. Triche.** 1987. Experimental evidence for a neural origin of Ewing's sarcoma of bone. Am. J. Pathol. **127:**507–518.
5. **Chang, L., Y. Jones, M. H. Ellisman, L. S. Goldstein, and M. Karin.** 2003. JNK1 is required for maintenance of neuronal microtubules and controls phosphorylation of microtubule-associated proteins. Dev. Cell **4:**521–533.
6. **Ciani, L., and P. C. Salinas.** 2005. WNTs in the vertebrate nervous system: from patterning to neuronal connectivity. Nat. Rev. Neurosci. **6:**351–362.
7. **Clevers, H.** 2006. Wnt/beta-catenin signaling in development and disease. Cell **127:**469–480.
8. **de Alava, E., and J. Pardo.** 2001. Ewing tumor: tumor biology and clinical applications. Int. J. Surg. Pathol. **9:**7–17.
9. **Endo, Y., and J. S. Rubin.** 2007. Wnt signaling and neurite outgrowth: insights and questions. Cancer Sci. **98:**1311–1317.
10. **Endo, Y., V. Wolf, K. Muraiso, K. Kamijo, L. Soon, A. Uren, M. Barshishat-Kupper, and J. S. Rubin.** 2005. Wnt-3a-dependent cell motility involves RhoA activation and is specifically regulated by dishevelled-2. J. Biol. Chem. **280:**777–786.
11. **Eom, D. S., W. S. Choi, S. Ji, J. W. Cho, and Y. J. Oh.** 2005. Activation of c-Jun N-terminal kinase is required for neurite outgrowth of dopaminergic neuronal cells. Neuroreport **16:**823–828.
12. **Fan, S., S. H. Ramirez, T. M. Garcia, and S. Dewhurst.** 2004. Dishevelled promotes neurite outgrowth in neuronal differentiating neuroblastoma 2A cells, via a DIX-domain dependent pathway. Mol. Brain Res. **132:**38–50.
13. **Giarré, M., M. V. Semenov, and A. M. Brown.** 1998. Wnt signaling stabilizes the dual-function protein beta-catenin in diverse cell types. Ann. N. Y. Acad. Sci. **857:**43–55.
14. **Hall, A. C., F. R. Lucas, and P. C. Salinas.** 2000. Axonal remodeling and synaptic differentiation in the cerebellum is regulated by WNT-7a signaling. Cell **100:**525–535.
15. **Keeble, T. R., M. M. Halford, C. Seaman, N. Kee, M. Macheda, R. B. Anderson, S. A. Stacker, and H. M. Cooper.** 2006. The Wnt receptor Ryk is required for Wnt5a-mediated axon guidance on the contralateral side of the corpus callosum. J. Neurosci. **26:**5840–5848.
16. **Kishida, S., H. Yamamoto, and A. Kikuchi.** 2004. Wnt-3a and Dvl induce neurite retraction by activating Rho-associated kinase. Mol. Cell. Biol. **24:** 4487–4501.
17. **Lipinski, M., K. Braham, I. Philip, J. Wiels, T. Philip, C. Goridis, G. M. Lenoir, and T. Tursz.** 1987. Neuroectoderm-associated antigens on Ewing's sarcoma cell lines. Cancer Res. **47:**183–187.
18. **Liu, Y., J. Shi, C. C. Lu, Z. B. Wang, A. I. Lyuksyutova, X. J. Song, and Y. Zou.** 2005. Ryk-mediated Wnt repulsion regulates posterior-directed growth of corticospinal tract. Nat. Neurosci. **8:**1151–1159.
19. **Lu, W., V. Yamamoto, B. Ortega, and D. Baltimore.** 2004. Mammalian Ryk is a Wnt coreceptor required for stimulation of neurite outgrowth. Cell **119:**97–108.
20. **Lucas, F. R., R. G. Goold, P. R. Gordon-Weeks, and P. C. Salinas.** 1998. Inhibition of GSK-3beta leading to the loss of phosphorylated MAP-1B is an early event in axonal remodelling induced by WNT-7a or lithium. J. Cell Sci. **111:**1351–1361.
21. **Lucas, F. R., and P. C. Salinas.** 1997. WNT-7a induces axonal remodeling and increases synapsin I levels in cerebellar neurons. Dev. Biol. **192:**31–44.
22. **Lyuksyutova, A. I., C. C. Lu, N. Milanesio, L. A. King, N. Guo, Y. Wang, J. Nathans, M. Tessier-Lavigne, and Y. Zou.** 2003. Anterior-posterior guidance of commissural axons by Wnt-frizzled signaling. Science **302:**1984–1988.
23. **Malaterre, J., R. G. Ramsay, and T. Mantamadiotis.** 2007. Wnt-Frizzled signalling and the many paths to neural development and adult brain homeostasis. Front. Biosci. **12:**492–506.
24. **Miller, J. R.** 2002. The Wnts. Genome Biol. **3:**REVIEWS3001.
25. **Montcouquiol, M., E. B. Crenshaw III, and M. W. Kelley.** 2006. Noncanonical Wnt signaling and neural polarity. Annu. Rev. Neurosci. **29:**363–386.
26. **Niehrs, C.** 2006. Function and biological roles of the Dickkopf family of Wnt modulators. Oncogene **25:**7469–7481.
27. **Noguera, R., T. J. Triche, S. Navarro, M. Tsokos, and A. Llombart-Bosch.** 1992. Dynamic model of differentiation in Ewing's sarcoma cells. Comparative analysis of morphologic, immunocytochemical, and oncogene expression parameters. Lab. Investig. **66:**143–151.
28. **Oliva, A. A., Jr., C. M. Atkins, L. Copenagle, and G. A. Banker.** 2006. Activated c-Jun N-terminal kinase is required for axon formation. J. Neurosci. **26:**9462–9470.
29. **Orme, M. H., A. L. Giannini, M. D. Vivanco, and R. M. Kypta.** 2003. Glycogen synthase kinase-3 and Axin function in a beta-catenin-independent pathway that regulates neurite outgrowth in neuroblastoma cells. Mol. Cell. Neurosci. **24:**673–686.
30. **Riggi, N., and I. Stamenkovic.** 2007. The biology of Ewing sarcoma. Cancer Lett. **254:**1–10.
31. **Rorie, C. J., V. D. Thomas, P. Chen, H. H. Pierce, J. P. O'Bryan, and B. E.**

Weissman. 2004. The Ews/Fli-1 fusion gene switches the differentiation program of neuroblastomas to Ewing sarcoma/peripheral primitive neuroectodermal tumors. Cancer Res. **64:**1266–1277.
32. **Rosso, S. B., D. Sussman, A. Wynshaw-Boris, and P. C. Salinas.** 2005. Wnt signaling through Dishevelled, Rac and JNK regulates dendritic development. Nat. Neurosci. **8:**34–42.
33. **Schmitt, A. M., J. Shi, A. M. Wolf, C. C. Lu, L. A. King, and Y. Zou.** 2006. Wnt-Ryk signalling mediates medial-lateral retinotectal topographic mapping. Nature **439:**31–37.
34. **Seifert, J. R., and M. Mlodzik.** 2007. Frizzled/PCP signalling: a conserved mechanism regulating cell polarity and directed motility. Nat. Rev. Genet. **8:**126–138.
35. **Shea, T. B.** 1999. Selective stabilization of microtubules within the proximal region of developing axonal neurites. Brain Res. Bull. **48:**255–261.
36. **Staege, M. S., C. Hutter, I. Neumann, S. Foja, U. E. Hattenhorst, G. Hansen, D. Afar, and S. E. Burdach.** 2004. DNA microarrays reveal relationship of Ewing family tumors to both endothelial and fetal neural crest-derived cells and define novel targets. Cancer Res. **64:**8213–8221.
37. **Uren, A., F. Reichsman, V. Anest, W. G. Taylor, K. Muraiso, D. P. Bottaro, S. Cumberledge, and J. S. Rubin.** 2000. Secreted frizzled-related protein-1 binds directly to Wingless and is a biphasic modulator of Wnt signaling. J. Biol. Chem. **275:**4374–4382.
38. **Uren, A., V. Wolf, Y. F. Sun, A. Azari, J. S. Rubin, and J. A. Toretsky.** 2004. Wnt/Frizzled signaling in Ewing sarcoma. Pediatr. Blood Cancer **43:**243–249.
39. **Votin, V., W. J. Nelson, and A. I. Barth.** 2005. Neurite outgrowth involves adenomatous polyposis coli protein and beta-catenin. J. Cell Sci. **118:**5699–5708.
40. **Wang, Y., N. Guo, and J. Nathans.** 2006. The role of Frizzled3 and Frizzled6 in neural tube closure and in the planar polarity of inner-ear sensory hair cells. J. Neurosci. **26:**2147–2156.
41. **Wang, Y., N. Thekdi, P. M. Smallwood, J. P. Macke, and J. Nathans.** 2002. Frizzled-3 is required for the development of major fiber tracts in the rostral CNS. J. Neurosci. **22:**8563–8573.
42. **Wang, Y., J. Zhang, S. Mori, and J. Nathans.** 2006. Axonal growth and guidance defects in Frizzled3 knock-out mice: a comparison of diffusion tensor magnetic resonance imaging, neurofilament staining, and genetically directed cell labeling. J. Neurosci. **26:**355–364.
43. **Wodarz, A., and R. Nusse.** 1998. Mechanisms of Wnt signaling in development. Annu. Rev. Cell Dev. Biol. **14:**59–88.
44. **Yu, X., and R. C. Malenka.** 2003. Beta-catenin is critical for dendritic morphogenesis. Nat. Neurosci. **6:**1169–1177.
45. **Zhang, X., J. Zhu, G. Y. Yang, Q. J. Wang, L. Qian, Y. M. Chen, F. Chen, Y. Tao, H. S. Hu, T. Wang, and Z. G. Luo.** 2007. Dishevelled promotes axon differentiation by regulating atypical protein kinase C. Nat. Cell Biol.
46. **Zhou, F. Q., and W. D. Snider.** 2005. Cell biology: GSK-3beta and microtubule assembly in axons. Science **308:**211–214.